Journal of Data Acquisition and Processing
ISSN: 1004-9037
https://sjcjycl.cn/
DOI: 10.5281/zenodo.778273

PERFORMANCE AND REHABILITATION OF BEAM-COLUMN CONNECTIONS WITH WEAK SHEAR

Nimbalkar Sunil Narayan[1]
Research Scholar, Department of Civil Engg., Sri Satya Sai University of Technology and Medical Sciences, Sehore, Madhya Pradesh.

Dr. Ajay Swarup[2]
Research Guide, Department of Civil Engg., Sri Satya Sai University of Technology and Medical Sciences, Sehore, Madhya Pradesh

Abstract
This experimental study investigated the behavior of beam-column connections with beams weak in shear. The experiment involved connections of varying sizes: full, two-thirds, and one-third size, subjected to loading types 1 and 2. Following testing, different rehabilitation strategies were employed based on the observed degree of damage. The rehabilitated specimens were then re-tested using the same loading sequence as the control specimens. Data collected during testing was utilized for post-processing to evaluate various parameters related to the seismic capacity of the connections. The performance of the rehabilitated specimens was examined and compared with that of the original, deficient control specimens. Bi-logarithmic plots were utilized to investigate the potential impact of size on ultimate strength, and correlations were established between specimen sizes, cumulative energy dissipation per unit volume of the D-region, and stresses. This comprehensive analysis sheds light on the behavior of beam-column connections with weak shear and provides insights into effective rehabilitation strategies.

Keywords: Beam-column connections, Weak shear, Rehabilitation techniques, Shear reinforcement

Introduction

Structural connections play a crucial role in ensuring the stability and safety of buildings and other structures. Among various types of connections, beam-column connections are of particular importance as they are responsible for transferring loads between beams and columns. However, beam-column connections are often vulnerable to shear failure, especially in regions with high seismic activity. When shear forces exceed the capacity of the connection, it can lead to significant structural damage or even collapse.

Weak shear in beam-column connections is a common issue that engineers and researchers have been addressing for decades. The term "weak shear" refers to the inadequate capacity of the connection to resist shear forces. This weakness can result from various factors such as insufficient reinforcement, poor detailing, material deterioration, or improper construction practices. Identifying, analyzing, and rehabilitating beam-column connections with weak shear are essential tasks to ensure the safety and resilience of structures, particularly in earthquake-prone regions.

Causes of Weak Shear in Beam-Column Connections

Several factors can contribute to weak shear in beam-column connections. Understanding these factors is essential for identifying vulnerable connections and implementing appropriate rehabilitation strategies. Some common causes of weak shear in beam-column connections include:

Insufficient Shear Reinforcement

One of the primary causes of weak shear in beam-column connections is insufficient shear reinforcement. Shear reinforcement, such as stirrups or ties, is essential for resisting shear forces and preventing diagonal cracking. Inadequate shear reinforcement can lead to premature failure of the connection under shear loading.

Inadequate Detailing

Poor detailing of beam-column connections can also contribute to weak shear. Inadequate lap splicing, improper anchorage of reinforcement, and inadequate concrete cover can reduce the shear capacity of the connection and compromise its performance.

Material Deterioration

Material deterioration, such as corrosion of reinforcement, can significantly affect the shear capacity of beam-column connections. Corrosion can weaken the reinforcement, reducing its ability to resist shear forces and increasing the vulnerability of the connection to shear failure.

Construction Deficiencies

Improper construction practices, such as inadequate compaction of concrete, improper placement of reinforcement, and poor quality control, can lead to weak shear in beam-column connections. These deficiencies can result in reduced bond strength between concrete and reinforcement, compromising the overall performance of the connection.

Seismic Loading

In regions with high seismic activity, beam-column connections are subjected to significant shear forces during earthquakes. Weak shear in these connections can lead to brittle failure modes, such as shear cracking and diagonal tension failure, posing a severe risk to the integrity of the structure.

Material and Method

This experimental study investigated beam-column connections with beams weak in shear. The experiment included connections of varying sizes: full, two-thirds, and one-third size. Control specimens were subjected to either loading type 1 or type 2.

After testing, we employed different rehabilitation strategies based on the observed degree of damage. We re-tested the rehabilitated specimens using the same loading sequence as the control specimens. The data collected during testing was then used for post-processing to evaluate several important parameters related to the seismic capacity of the connections.

The performance of the rehabilitated specimens was examined and compared with that of the original, deficient control specimens. We also drew bi-logarithmic plots to investigate the potential impact of size on ultimate strength. Furthermore, we correlated the specimen sizes with the cumulative energy dissipated per unit volume of the D-region and stresses. This comprehensive analysis sheds light on the behavior of beam-column connections with weak shear and provides insights into effective rehabilitation strategies.

Response of Connections to Applied Loads: Type-1 Analysis

Figure 1 provides a close-up view of the joint region, showing the development of cracks during testing. At this stage, the specimens reached their peak capacities. Observing these figures, it becomes apparent that the initiation and propagation of cracks, both before and after repair, followed a similar pattern overall.

Both the control and rehabilitated specimens displayed a pattern where the first crack became visible in the beam part when the displacement amplitude reached approximately 5.0 mm. As the displacement amplitude increased, more cracks began to develop in both the beam and the joint region. Figure 2 shows the condition of the specimens at the end of the test.

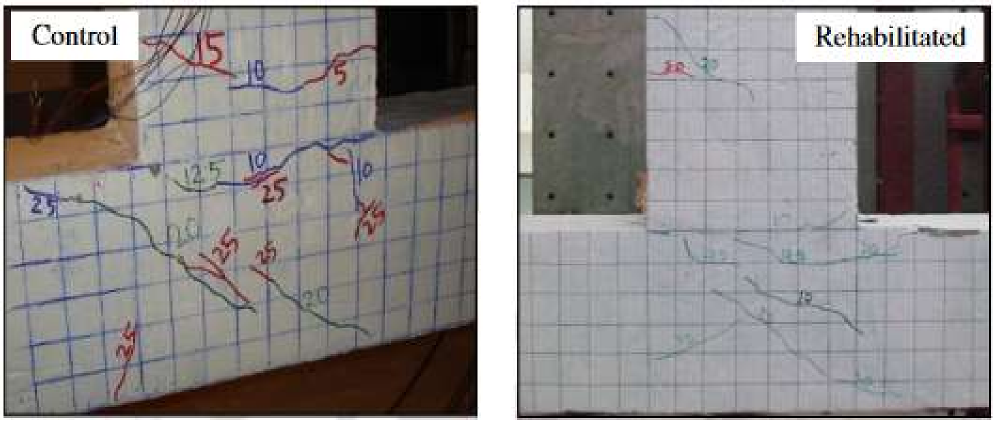

Figure 1. Observation of Cracks in BWSL Specimens under Type-1 Loading at Peak Load

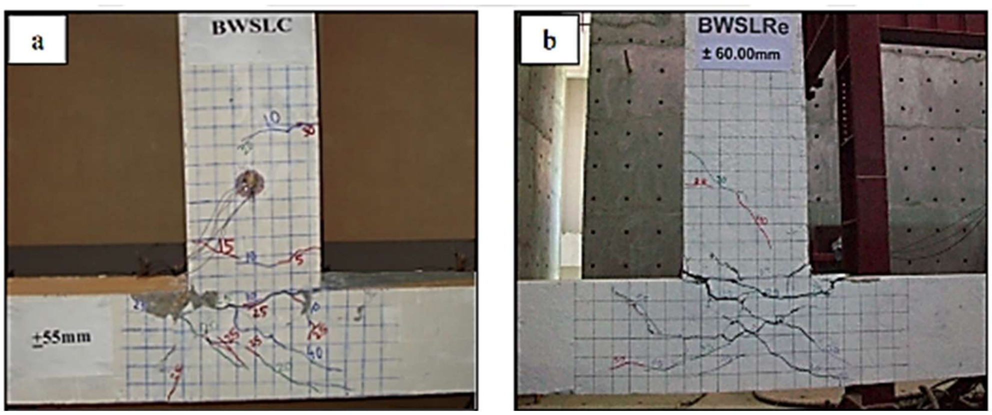

Figure 2. Control versus Rehabilitated BWSL Specimens under Loading Type-1

For the BWSLC specimen, the maximum load-carrying capacity was 70.78 kN in the push direction at the 22nd cycle with a displacement of 30 mm. At the 19th cycle, it reached 73.39 kN with a displacement of 25 mm in the pull direction.

Comparatively, the BWSLRe specimen showed a slightly higher load-carrying capacity than the control specimen in both push and pull directions. It reached a maximum load of 76.12 kN in the push direction at the 22nd cycle with a 30 mm displacement and at the 25th cycle with a 35 mm displacement.

In the control specimen, initial cracks widened when the peak load was attained. Concrete spalling at the joint region occurred at a displacement amplitude of ± 40 mm. At ± 50 mm displacement, existing cracks widened further, with a 6 mm-wide crack visible at the joint interface. The ultimate load-carrying capacity for the BWSLC specimen was found to be 72.085 kN.

For the rehabilitated specimen, hairline cracks at the joint region widened to about 1 mm at a ± 35 mm displacement. Until the peak loading stage, most cracks were concentrated in the joint region. The repair materials prevented early cracking of the joint interface. At a ± 50 mm displacement, cracks in the joint region widened to about 5 mm, and concrete crushing began at the joint interface, with some cracks propagating towards the column and beam regions.

Similar damage patterns were observed for both the control and rehabilitated specimens at the same displacement levels. However, the rehabilitated specimen was still capable of carrying additional load at a ± 55 mm displacement level, where the test for the control specimen was stopped. The experiment for the rehabilitated specimen was halted at ± 60 mm for safety, with the maximum load for the BWFLRe specimen found to be 77.220 kN.

Response of Connections to Applied Loads: Type-2 Analysis

We made significant observations regarding crack appearances and specimen damage during the testing. The initial crack was visible in the beam part of both the control and rehabilitated specimens at a displacement amplitude of ± 5.0 mm. As the displacement increased, more cracks emerged at the joint region and beam part, as depicted in Figure 3. In particular, cracks initially developed at the joint interface of the control specimen widened to approximately 1 mm when the displacement reached ± 25 mm. Interestingly, at the same displacement level, the rehabilitated specimen exhibited similar levels of damage.

This indicates that both the control and rehabilitated specimens experienced comparable damage patterns under similar displacement conditions. Such observations are critical for understanding the behavior of specimens under load and assessing the effectiveness of rehabilitation efforts. As you can see in Figure. 5, the hysteresis loops show how the control and rehabilitated specimens moved when they were loaded in different ways. The control specimen reached its maximum load of 76.63 kN during push displacement of 40 mm and 71.49 kN during pull displacement of 35 mm.

The rehabilitated specimen, however, showed slightly higher loads, reaching a maximum of 86.5 kN during push displacement and 75.44 kN during pull displacement, both at ±45 mm displacement amplitude. As the displacement increased, cracks at the joint interface widened to about 5 mm. At a ±50 mm displacement, there was a noticeable degradation in load-carrying capacity, leading to the experiment being stopped for the control specimen at a ±55 mm displacement.

For the BWSLC specimen, the ultimate load-carrying capacity was 74.06 kN. Damage patterns in the rehabilitated specimens were similar to those in the control specimen, with most cracks concentrated at the joint interface. At ±45 mm of displacement, concrete crushing at the joint interface began. As the displacement increased to ±50 mm, existing crack widths widened to about 3 mm. Although the rehabilitated specimen showed more cracks in the joint region compared to the control specimen at the same displacement level, it could be loaded up to ±60 mm with a maximum load-carrying capacity of 80.98 kN. Both the control and rehabilitated specimens had the same displacement limits under loading types 1 and 2. This made it easier to compare how they behaved based on the number of cycles of displacement history. Both the control and rehabilitated specimens showed a crack width of about 5 mm at the joint interface at the end of the test.

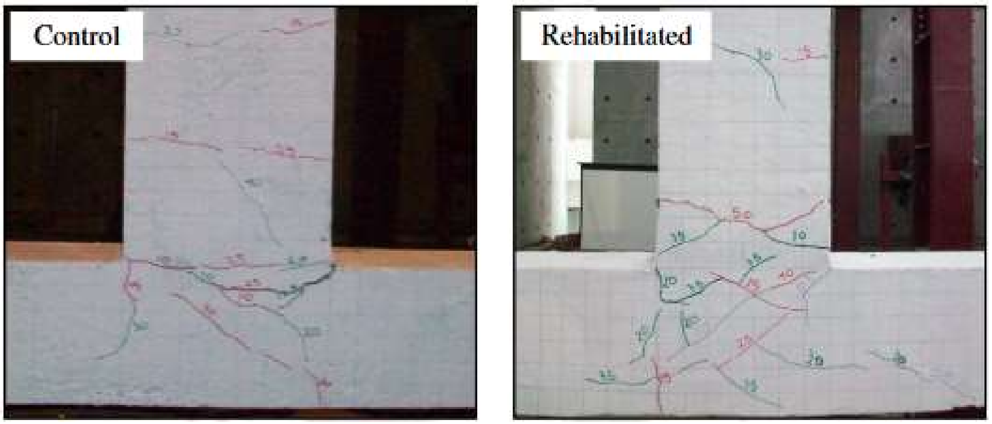

Figure 3. Observation of Cracks in BWSL Specimens under Type-2 Loading at Peak Load

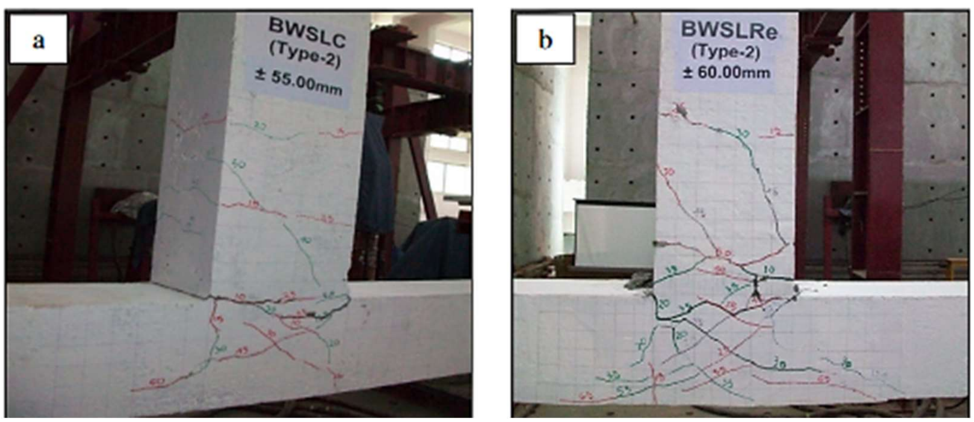

Figure 4. Control versus Rehabilitated BWSL Specimens under Loading Type-2

Result and Discussion

In the preceding sections, we've delved into the intricate dynamics of hysteretic responses across all connections. These responses serve as critical indicators for seismic capacity, revealing essential parameters like ultimate strength, stiffness degradation, energy dissipation, and ductility of the specimens. Through a thorough evaluation, we've assessed the efficacy of adopted repair techniques by juxtaposing the seismic performance of rehabilitated specimens against their unaltered counterparts.

These evaluations provide invaluable insights into the effectiveness of repair strategies in enhancing the structural resilience of specimens under seismic stress. By scrutinizing the comparative performance, we can discern the tangible impact of repair interventions on key seismic capacity metrics. This comprehensive analysis not only emphasizes the significance of proactive measures in mitigating seismic vulnerabilities, but also informs future strategies for bolstering structural robustness in the face of seismic challenges.

The hysteresis loops depicted in Figures 5 and 6 illustrate the control and rehabilitated specimens' behavior under various loading conditions. Analyzing these curves at different displacement levels reveals a notable trend: the rehabilitated specimens exhibit similar load-displacement characteristics, albeit with a slightly lower initial slope compared to their control counterparts. Despite this, the envelope of hysteresis loops for the rehabilitated specimens demonstrates a slightly higher load carrying capacity in both push and pull directions.

This observation suggests that the rehabilitation process effectively restores the load carrying capacity of damaged specimens. Notably, all damaged control specimens were able to regain their load carrying capacity following rehabilitation. Moreover, it's interesting to note that while the ultimate load carrying capacity of control specimens under loading types 1 and 2 remains comparable, slight differences in peak push and pull loads were observed.

This implies that the nature of applied loading doesn't significantly influence the ultimate load carrying capacity of specimens. However, when it comes to comparing the ultimate load carrying capacity of rehabilitated specimens under different loading types, it's challenging due to the application of varied rehabilitation strategies.

Nevertheless, the study underscores the effectiveness of appropriately chosen repair strategies in recovering lost capacity, even in severely damaged structural components. Consequently, it can be inferred that the applied repair techniques play a crucial role in restoring the load carrying capacity of critical beam-column connections, thereby ensuring structural integrity and safety.

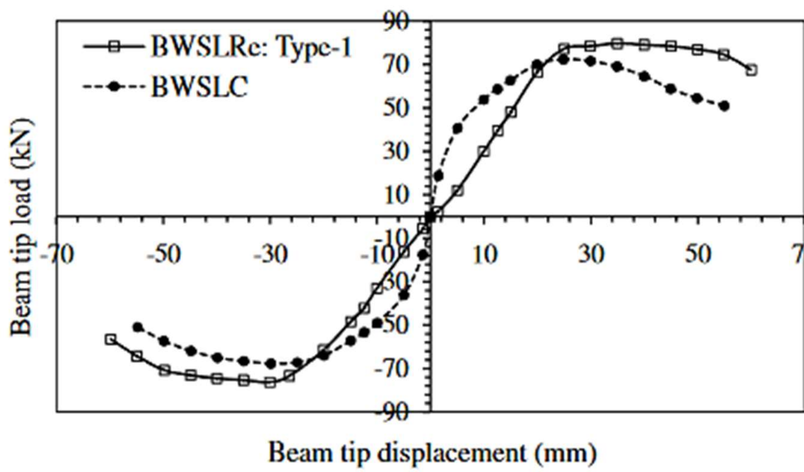

Figure 5. Envelope Curves Analysis of Specimens Subjected to Loading Type-1

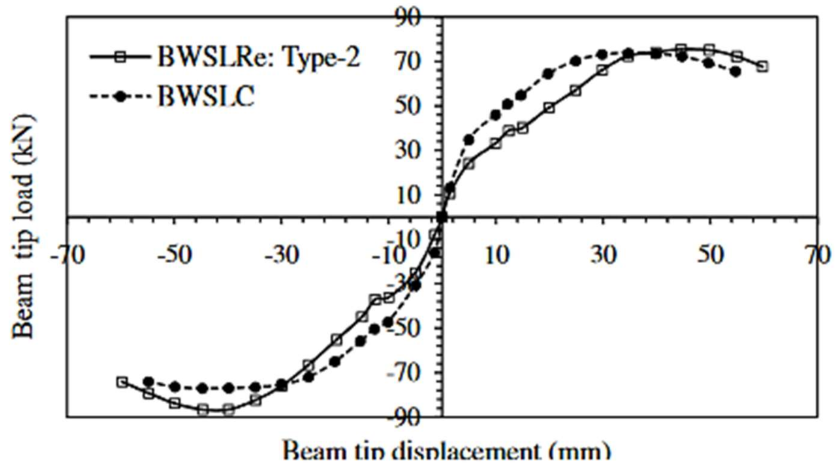

Figure 6. Envelope Curves Analysis of Specimens Subjected to Loading Type-2

Conclusion

The study provides critical insights into the seismic performance of beam-column connections with weak shear, as well as the efficacy of rehabilitation strategies. The hysteresis loops illustrated the behavior of control and rehabilitated specimens under various loading conditions. The rehabilitated specimens exhibited similar load-displacement characteristics to control specimens, albeit with a slightly lower initial slope. However, the envelope of hysteresis loops for the rehabilitated specimens demonstrated a slightly higher load carrying capacity in both push and pull directions. This indicates that the rehabilitation process effectively restored the load carrying capacity of damaged specimens. The study underscores the effectiveness of appropriately chosen repair strategies in recovering lost capacity, even in severely damaged structural components, ensuring structural integrity and safety.

References

1. G. E. Thermou, S. J. Pantazopoulou, and A. S. Elnashai, "Flexural behavior of brittle RC members rehabilitated with concrete jacketing," Journal of Structural Engineering, vol. 133, no. 10, pp. 1373–1384, 2007.
2. S. N. Bousias, D. Biskinis, M. N. Fardis, and A. L. Spathis, "Strength, stiffness, and cyclic deformation capacity of concrete jacketed members," ACI Structural Journal, vol. 104, no. 5, pp. 521–531, 2007.
3. F. Altun, "An experimental study of the jacketed reinforced-concrete beams under bending," Construction and Building Materials, vol. 18, no. 8, pp. 611–618, 2004.
4. G. Tsonos, "Lateral load response of strengthened reinforced concrete beam-to-column joints," ACI Structural Journal, vol. 96, no. 1, pp. 46–56, 1999.
5. K. G. Vandoros and S. E. Dritsos, "Concrete jacket construction detail effectiveness when strengthening RC columns," Construction and Building Materials, vol. 22, no. 3, pp. 264–276, 2008.
6. D. G. Tsonos, "Performance enhancement of R/C building columns and beam-column joints through shotcrete jacketing," Engineering Structures, vol. 32, no. 3, pp. 726–740, 2010.

7. G. E. Thermou, S. J. Pantazopoulou, and A. S. Elnashai, "Global interventions for seismic upgrading of substandard RC buildings," Journal of Structural Engineering, vol. 138, no. 3, pp. 387–401, 2012.
8. T. Georgopoulos and S. E. Dritsos, "A steel jacketing technique for strengthening RC columns," in Proceedings of the 10th European Conference on Earthquake Engineering, pp. 2275–2280, Vienna, Austria, 1994.
9. C. E. Chalioris, "Torsional strengthening of rectangular and flanged beams using carbon fibre-reinforced-polymers—experimental study," Construction and Building Materials, vol. 22, no. 1, pp. 21–29, 2008.
10. C. G. Karayannis and G. M. Sirkelis, "Strengthening and rehabilitation of RC beam-column joints using carbon-FRP jacketing and epoxy resin injection," Earthquake Engineering and Structural Dynamics, vol. 37, no. 5, pp. 769–790, 2008.
11. T. C. Triantafillou and C. G. Papanicolaou, "Shear strengthening of reinforced concrete members with textile reinforced mortar (TRM) jackets," Materials and Structures, vol. 39, no. 285, pp. 93–103, 2006.
12. D. A. Bournas and T. C. Triantafillou, "Flexural strengthening of reinforced concrete columns with near-surface-mounted FRP or stainless steel," ACI Structural Journal, vol. 106, no. 4, pp. 495–505, 2009.
13. C. G. Karayannis, C. E. Chalioris, and G. M. Sirkelis, "Local retrofit of exterior RC beam-column joints using thin RC jackets—an experimental study," Earthquake Engineering and Structural Dynamics, vol. 37, no. 5, pp. 727–746, 2008.
14. K. H. Khayat, "Workability, testing, and performance of self-consolidating concrete," ACI Materials Journal, vol. 96, no. 3, pp. 346–353, 1999.
15. S. Georgiadis, K. K. Sideris, and N. S. Anagnostopoulos, "Properties of scc produced with limestone filler or viscosity modifying admixture," Journal of Materials in Civil Engineering, vol. 22, no. 4, pp. 352–360, 2010.
16. T. Albanesi, D. Lavorato, C. Nuti, and S. Santini, "Experimental tests on repaired and retrofitted bridge piers," in Proceedings of the International FIB Symposium, pp. 673–678, Amsterdam, The Netherlands, 2008.
17. C. G. Fakitsas, P. E. A. Papakonstantinou, P. D. Kiousis, and A. Savva, "Effects of recycled concrete aggregates on the compressive and shear strength of high-strength self-consolidating concrete," Journal of Materials in Civil Engineering, vol. 24, no. 4, pp. 356–361, 2012.
18. K. M. Heiza, N. N. Meleka, and N. Y. Elwkad, "Behavior and analysis of self-consolidated reinforced concrete deep beams strengthened in shear," Journal of ISRN Civil Engineering, vol. 2012, Article ID 202171, 14 pages, 2012.
19. K. K. Sideris, A. S. Georgiadis, N. S. Anagnostopoulos, and P. Manita, "Low strength self compacting concrete for building application," in Proceedings of the International FIB Symposium, pp. 1057–1059, Amsterdam, The Netherlands, 2008.
20. C. G. Karayannis, C. E. Chalioris, and K. K. Sideris, "Effectiveness of RC beam-column connection repair using epoxy resin injections," Journal of Earthquake Engineering, vol. 2, no. 2, pp. 217–240, 1998.